PROCEEDINGS OF SCIENCE

D-Egg: a Dual PMT Optical Module for the IceCube Upgrade

The IceCube Collaboration
(a complete list of authors can be found at the end of the proceedings)

E-mail: colton.hill@icecube.wisc.edu, max.meier@icecube.wisc.edu, ryo.nagai@icecube.wisc.edu

The D-Egg, a dual PMT optical sensor, is one of the new optical modules designed for the coming IceCube Upgrade at the South Pole. With two 8-inch high-quantum efficiency photomultiplier tubes (PMTs) per module and improvements in overall design, D-Eggs offer an increased effective photodetection sensitivity that is 2.8 times larger than that of the current IceCube optical sensors. Mass production of over 300 D-Eggs has been completed, with all modules now undergoing Final Acceptance Testing (FAT) before deployment in the Antarctic ice. This involves detailed characterisation of each module at cold temperatures to collect valuable calibration data, as well as detect possible hardware related failures. While FAT is still on-going, current results indicate we will exceed the required 277 modules for deployment.

Corresponding authors: Colton Hill[1*], Maximilian Meier[1], Ryo Nagai[1]
[1] *Chiba University, Department of Physics and The International Center for Hadron Astrophysics, 1-33 Yayoicho, Chiba, Japan*

[*] Presenter

38th International Cosmic Ray Conference (ICRC2023)
26 July - 3 August, 2023
Nagoya, Japan

PoS(ICRC2023)1082

1. IceCube & the IceCube Upgrade

The IceCube Neutrino Observatory is at the geographic South Pole and has been fully operational since 2011 [1]. The instrumented volume encompasses roughly 1 km^3 of highly transparent glacial ice, which is sparsely filled with chains of digital optical modules (DOMs) extending down to depths of 2450 m from the surface. Resulting particles from neutrino interactions in the ice create Cherenkov radiation as they propagate. This Cherenkov radiation is detected by the photo-multiplier tubes (PMTs) inside the glass housings of the optical modules and is transmitted to IceCube facilities located on the ice surface, before being transmitted via satellite to the northern hemisphere for offline analysis.

Following over 10 years of consistent operation and discoveries [2–7], a new set of modules will be deployed into the Antarctic ice as part of the IceCube Upgrade. As part of the IceCube Upgrade a mixture of calibration and physics devices will further populate the densely-instrumented inner detector area, as seen in Figure 1. Each "string", the chain of modules inserted into the hole, will be primarily instrumented with a combination of two modules specifically designed as successors to the successful first generation DOM design, the "mDOM" and the "D-Egg". The following sections will focus primarily on the design and performance of the D-Egg [8], including a significant increase in tested modules since our publication in April 2023. Please see other proceedings for more details on the mDOM [9].

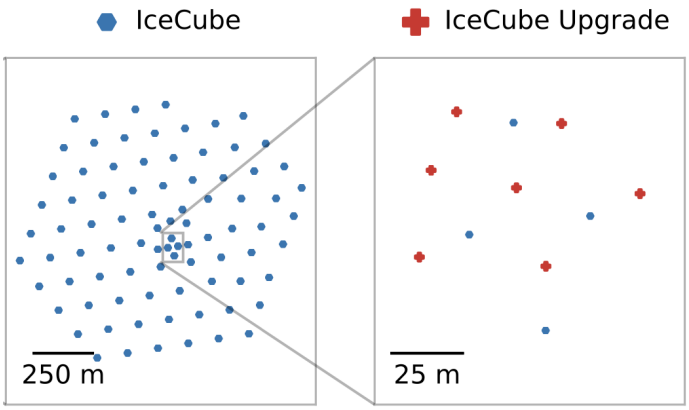

Figure 1: Layout of deployed IceCube Gen1 string locations (left) and proposed layout of IceCube Upgrade string locations (right) [10]. The more densely populated inner detector region will further enhance MeV & GeV-scale sensitivitiy.

2. From DOM to D-Egg

IceCube Gen1 DOMs are composed of a single downward-facing 10-inch diameter PMT and readout electronics located inside an evacuated glass vessel [1]. The D-Egg (Figure 2) further develops the simple, but robust, Gen1 DOM design in key areas such as calibration versatility [11], cost effectiveness, and photo-detection efficiency. One of the key features are the replacement of the single 10-inch downward-facing PMT (HPK R7081-02) with a pair of opposite-facing 8-inch high

quantum efficiency PMTs (HPK R5912-100-70). Improvements in the glass and optical coupling gel transparency to sub-400 nm Cherenkov light combined with the high quantum efficiency PMTs leads to factor 2.8 improvement in effective area compared to the Gen1 DOMs. Comparisons of the D-Egg to Gen1 DOM effective area at 320 nm, 400 nm, and averaged over the Cherenkov spectrum are shown in Figure 3 [8] For more specifics regarding component improvements see [8].

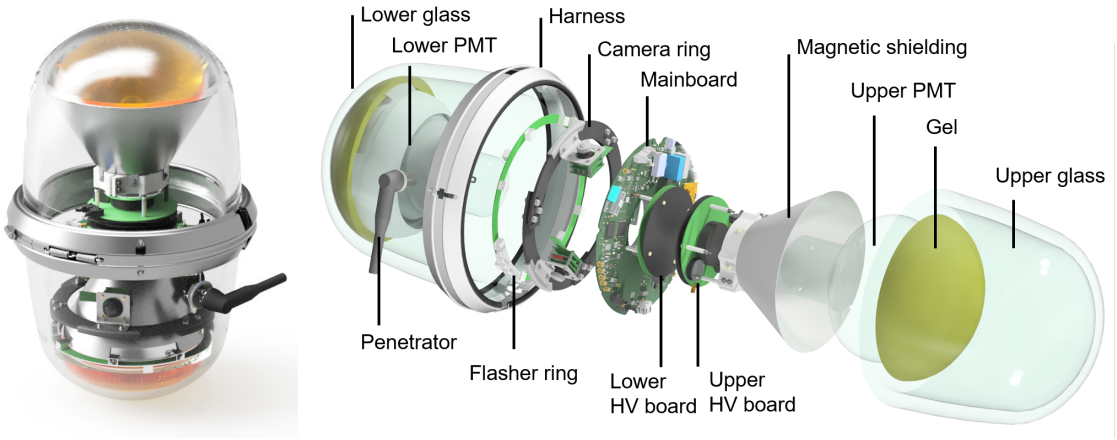

Figure 2: (Left) An assembled D-Egg. (Right) Exploded D-Egg showing the glass housing, mainboard, calibration devices (cameras and LED flashers), PMTs, optical coupling silicone (gel), and magnetic shielding (FINEMET®) [8].

3. Laboratory Testing & Performance

As part of the expanded IceCube Upgrade array, 277 of the 310 constructed D-Eggs are planned for deployment. In order to verify the performance of each module prior to shipping to the South Pole, each module undergoes a series of calibration and characterisation tests inside our Final Acceptance Testing (FAT) freezer. Limited by the capacity of the freezer, D-Eggs are tested in batches of 16 over a 3 week duration. A module spends around 80% of its time below zero, reaching a minimum temperature of −40 °C. This meets the expected coldest temperature a module will operate at once deployed in the ice. Since publication of [8], over 100 additional modules have been tested providing a wider scope of the D-Egg bulk behaviour. Modules have been sampled randomly from the production, to detect possible defects related to when the module was assembled. Quantities particularly important to in-ice operations are the per PMT dark rate, and the per PMT single photo-electron timing resolution.

3.1 Testing Procedure

Each D-Egg is continuously operated during the FAT period, during which integrated several hours of low-threshold triggers per PMT are collected in order to perform calibration of the PMT gain, as well as investigate the dark rate. When operating during a period of constant temperature, the PMT high voltage is held constant in order to evaluate the stability of a module. Tests which require

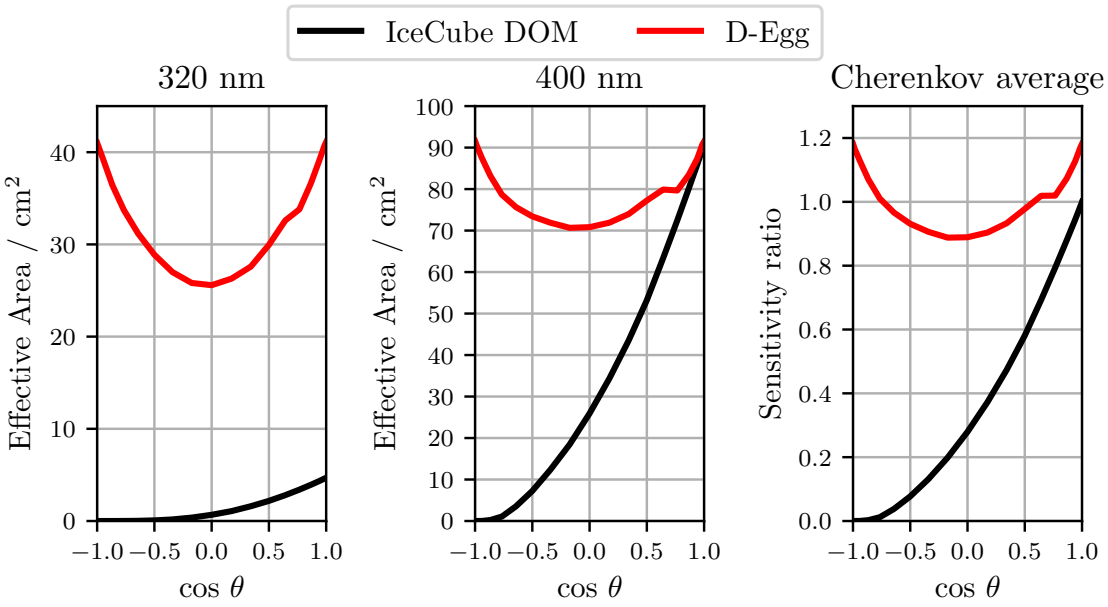

Figure 3: Comparison between the D-Egg and the Gen1 DOM as a function of the cosine of the zenith angle of the incident photons. Improvements in the detection uniformity are largely driven by moving from a single to multiple PMTs. The effective area is calculated at 320 nm (left), 400 nm (center), and the Cherenkov-averaged sensitivity ratio (right), with the downward-facing direction defined as $\theta = 0$ ($\cos\theta = 1$).

external light injection are performed simultaneously for each PMT with light delivered via optical fibres from a primary 400 nm picosecond laser [1].

The stability, dark rate, and timing resolution, among other quantities are evaluated on a per module basis to determine if a D-Egg is suitable for deployment. FAT testing is still in-progress, with a total of 143 modules, corresponding to 286 PMTs, having finished testing as of June 2023. Results below report the current status as of this point. Testing of all 310 modules should finish by Spring of 2024, well-ahead of the Upgrade deployment season (2025/2026).

3.2 Dark Rate

The per PMT dark rate is a critical quantity for controlling the in-ice false trigger rate, as the current Gen1 IceCube trigger relies heavily on inter-module coincidence signals. The decay of ^{40}K in the borosilicate glass pressure vessel enclosing the D-Egg as well as the PMT thermionic emissions (which are a function of temperature) are the primary contributions to the dark rate. More complex trigger schema including intra-module coincidence triggers are also being considered for the IceCube Upgrade. This makes particularly the mean dark rate per module an important quantity to compare between the Gen1 DOM and D-Egg.

The dark rate is collected per PMT by requiring the average of two consecutive waveform bins to exceed a threshold of 0.25 PE, where 1 PE is the peak height of the average SPE pulse. An artificial dead time of 100 ns is applied to prevent recording multiple triggers from the same pulse. As D-Eggs during FAT testing operate in air (not ice), an experimentally determined dark rate

[1] https://www.hamamatsu.com/resources/pdf/sys/SOCS0003E_PLP-10.pdf

correction factor of 2.37, due to differences in the glass:air & glass:ice refractive index, is applied to results shown here [8, 12].

The collective per PMT dark rate as well as the per D-Egg dark rate are shown in Figure 4, with an average dark rate of 917 ± 100 Hz per PMT and 1835 ± 155 Hz per module. On average the Gen1 DOM has a dark rate of 870 Hz, which can be compared to the D-Egg dark rate by normalising by the ratio of the Cherenkov-averaged effective areas, resulting in 655 Hz. In order to compare results consistently between D-Eggs tested in different FAT runs, the values are quoted with each module operating at nominal gain and during the same period during each FAT cycle with the freezer set to -40 °C.

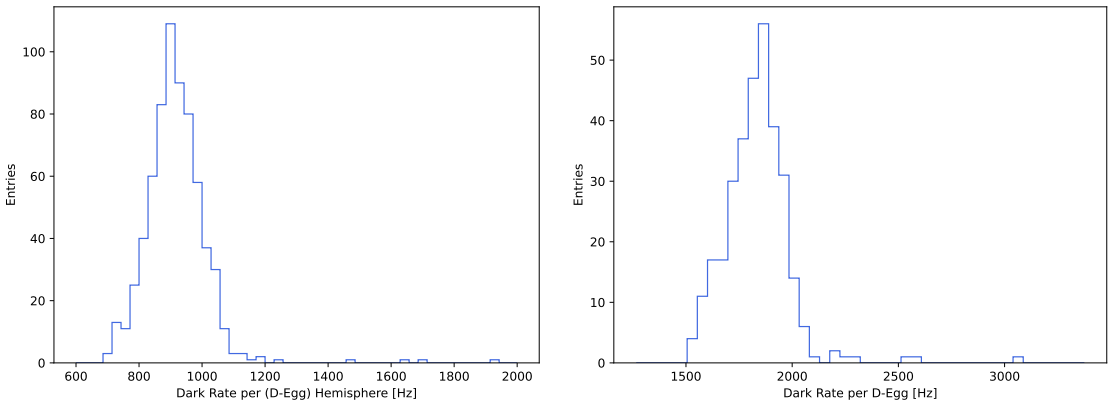

Figure 4: Dark rate per PMT (left), and dark rate per D-Egg (right), at -40 °C ambient temperature.

3.3 Timing Resolution

Typical number of photons observed by individual optical modules in IceCube is on the order of only a few for all but the highest energy events. In this case, the timing resolution for identifying a single photo-electron is extremely important. For each D-Egg, both the top and bottom PMTs are illuminated with a 1 kHz pulsed laser calibrated to a single photo-electron light level. The sync-out signal published by the laser is digitised and used to determine the emission time. Triggers in the PMT which are temporally consistent with the sync-out populate the transit time distribution, from which the single photon timing resolution (SPTR) is extracted. Figure 5 shows the per PMT resolution and the boundary for the acceptance criteria in yellow. The average per PMT SPTR of 2.84 ± 0.11 ns indicates that D-Eggs should be able to competently resolve SPE-level interactions at distances only a few 10s of metres away from any given module [8].

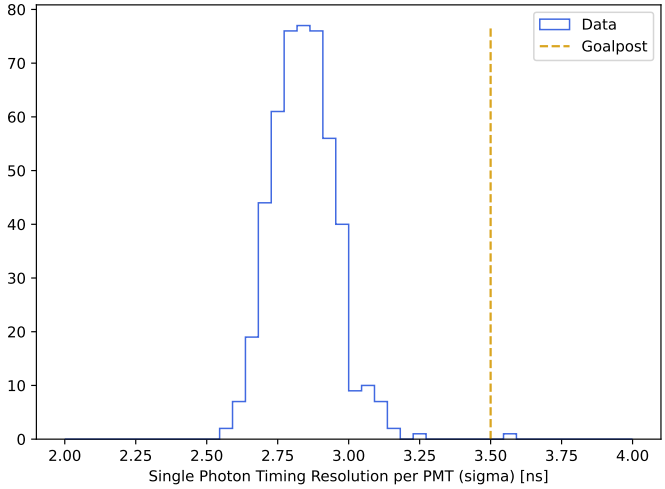

Figure 5: Per PMT single photon timing resolution (SPTR) determined at −40 °C ambient temperature. The yellow line indicates the upper-bound for acceptable timing resolutions to sufficiently resolve characteristic interactions in IceCube at distances around 30 m [8].

3.4 Long-term Stability Performance

As a part of the on-going FAT testing, a well-tested D-Egg has remained inside the freezer for all 9 runs (21 weeks) included in these proceedings. The PMTs of this module were verified prior to FAT testing to have behaviour consistent with modules which pass the acceptance testing. While various parameters are monitored throughout one FAT cycle, distributions of the stability corresponding to the distributions discussed in Sections 3.2 and 3.3 are included as Figures 6 and 7.

The dark rate results in Figure 6 were collected at −40 °C ambient temperature, in the same manner as described in Figure 4. For the channel 0 PMT, the mean dark rate is 892 ± 13 Hz and 959 ± 10 Hz for the channel 1 PMT. These results are consistent with the results observed for the range of modules tested so-far. Additionally, no trends in the dark rate have been observed which may indicate systematic bias in the testing apparatus or hardware failure.

Examining the stability of the SPTR provides additional context for the stability of the light injection system as a part of the FAT setup. No long term trends have been observed in the SPTR for either channel (Figure 7) with mean SPTR for the channel 0 PMT at 2.84 ± 0.08 ns and 2.88 ± 0.08 ns for the channel 1 PMT. Fluctuations in the cycle-by-cycle resolution reveal the precision of the system, as the PMT timing resolution during continuous operation are expected to be constant.

Considering the results for the dark rate and SPTR, the reference module has operated stably for over 9 months and has continuous performance which is representative of the broader D-Egg PMT bulk behaviour. This module is additionally a practical demonstration that the design of the D-Egg is robust with respect to long-term operations and temperature variations far more extreme than that experienced in the South Pole ice.

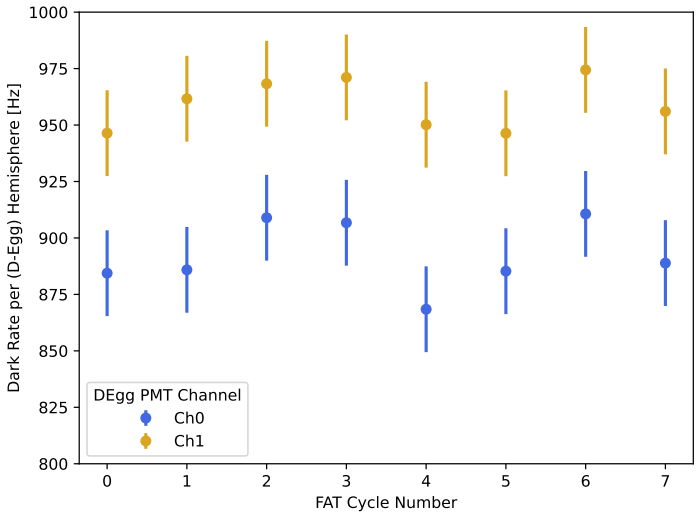

Figure 6: Dark rate per (D-Egg) hemisphere at −40 °C ambient temperature for the two PMTs in the reference D-Egg module versus FAT cycle number. Lack of drift in dark rates towards either higher or lower values indicates stability of the D-Egg hardware as well as the FAT setup.

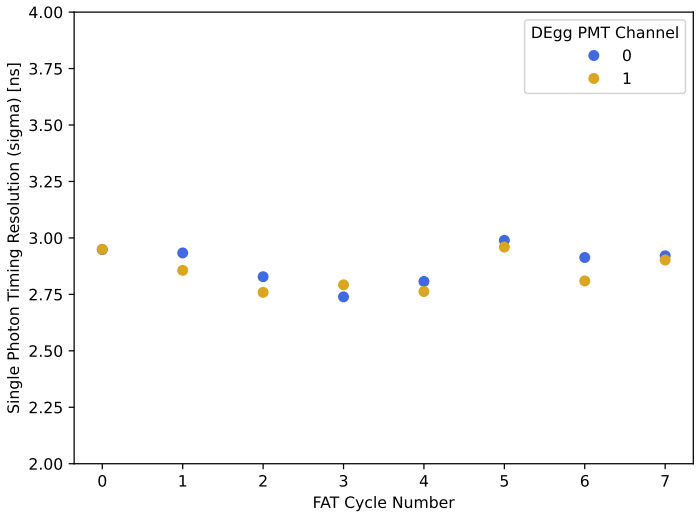

Figure 7: Single photon timing resolution (SPTR) determined at −40 °C ambient temperature for the reference D-Egg PMTs. Variations in the resolution of either PMT are driven by the precision of the measurement.

4. Outlook

To enhance IceCube's current physics goals and provide an opportunity for in-field testing of new novel devices, the IceCube Upgrade will see a number of new detectors deployed into the South Pole ice during the 2025/2026 season [13]. One of these new devices, the D-Egg, has finished production of 310 modules and is currently in the mass-testing phase prior to deployment in the Antarctic ice. Improvements in design and careful selection of components have resulted in a net

increase in effective area per module of 2.8 times over the first generation IceCube DOMs.

Final Acceptance Testing for the D-Eggs is planned to finish in Spring 2024, having characterised over 600 PMTs with a broad suite of measurements. Tests highlighted here, the PMT dark rate and single photon timing resolution, are two key quantities which determine whether a module is suitable for deployment. Measurements by the reference D-Egg indicate stability across FAT cycles and at this stage, the majority of modules satisfy the requirements discussed here. Current performance projects satisfying the required number of D-Eggs for IceCube Upgrade deployment.

References

[1] **IceCube** Collaboration, M. G. Aartsen *et al.* *JINST* **12** no. 03, (2017) P03012.

[2] **IceCube** Collaboration, M. G. Aartsen *et al.* *Phys. Rev. Lett.* **124** no. 5, (2020) 051103.

[3] **IceCube** Collaboration, R. Abbasi *et al.* *Science* **378** no. 6619, (2022) 538–543.

[4] **IceCube** Collaboration, M. G. Aartsen *et al.* *Nature* **551** (2017) 596–600.

[5] **IceCube** Collaboration, M. G. Aartsen *et al.* *Nature* **591** no. 7849, (2021) 220–224. [Erratum: Nature 592, E11 (2021)].

[6] **IceCube** Collaboration, M. Aartsen *et al.* *Phys. Rev. Lett* **120** (2018) 071801.

[7] **IceCube** Collaboration, M. Aartsen *et al.* *Phys. Rev. D* **99** (2019) 032007.

[8] **IceCube** Collaboration, R. Abbasi *et al.* *Journal of Instrumentation* **18** no. 04, (Apr, 2023) P04014.

[9] **IceCube-Gen2** Collaboration, L. Classen, M. Kossatz, A. Kretzschmann, S. Lindner, and D. Shuklin *PoS* **ICRC2017** (2018) 1047.

[10] **IceCube** Collaboration, M. Aartsen *et al.* *Journal of Physics G: Nuclear and Particle Physics* **48** no. 6, (Apr, 2021) 060501.

[11] **IceCube** Collaboration, A. Ishihara and A. Kiriki *PoS* **ICRC2019** (2019) 923.

[12] **IceCube** Collaboration, C. Hill *et al.*, "Performance of the D-Egg Optical Sensor for the IceCube Upgrade," in *37th International Cosmic Ray Conference*. 8, 2021. arXiv:2108.05353 [physics.ins-det].

[13] **IceCube** Collaboration, A. Ishihara *PoS* **ICRC2019** (2021) 1031.

Full Author List: IceCube Collaboration

R. Abbasi[17], M. Ackermann[63], J. Adams[18], S. K. Agarwalla[40, 64], J. A. Aguilar[12], M. Ahlers[22], J.M. Alameddine[23], N. M. Amin[44], K. Andeen[42], G. Anton[26], C. Argüelles[14], Y. Ashida[53], S. Athanasiadou[63], S. N. Axani[44], X. Bai[50], A. Balagopal V.[40], M. Baricevic[40], S. W. Barwick[30], V. Basu[40], R. Bay[8], J. J. Beatty[20, 21], J. Becker Tjus[11, 65], J. Beise[61], C. Bellenghi[27], C. Benning[1], S. BenZvi[52], D. Berley[19], E. Bernardini[48], D. Z. Besson[36], E. Blaufuss[19], S. Blot[63], F. Bontempo[31], J. Y. Book[14], C. Boscolo Meneguolo[48], S. Böser[41], O. Botner[61], J. Böttcher[1], E. Bourbeau[22], J. Braun[40], B. Brinson[6], J. Brostean-Kaiser[63], R. T. Burley[2], R. S. Busse[43], D. Butterfield[40], M. A. Campana[49], K. Carloni[14], E. G. Carnie-Bronca[2], S. Chattopadhyay[40, 64], N. Chau[12], C. Chen[6], Z. Chen[55], D. Chirkin[40], S. Choi[56], B. A. Clark[19], L. Classen[43], A. Coleman[61], G. H. Collin[15], A. Connolly[20, 21], J. M. Conrad[15], P. Coppin[13], P. Correa[13], D. F. Cowen[59, 60], P. Dave[6], C. De Clercq[13], J. J. DeLaunay[58], D. Delgado[14], S. Deng[1], K. Deoskar[54], A. Desai[40], P. Desiati[40], K. D. de Vries[13], G. de Wasseige[37], T. DeYoung[24], A. Diaz[15], J. C. Díaz-Vélez[40], M. Dittmer[43], A. Domi[26], H. Dujmovic[40], M. A. DuVernois[40], T. Ehrhardt[41], P. Eller[27], E. Ellinger[62], S. El Mentawi[1], D. Elsässer[23], R. Engel[31, 32], H. Erpenbeck[40], J. Evans[19], P. A. Evenson[44], K. L. Fan[19], K. Fang[40], K. Farrag[16], A. R. Fazely[7], A. Fedynitch[57], N. Feigl[10], S. Fiedlschuster[26], C. Finley[54], L. Fischer[63], D. Fox[59], A. Franckowiak[11], A. Fritz[41], P. Fürst[1], J. Gallagher[39], E. Ganster[1], A. Garcia[14], L. Gerhardt[9], A. Ghadimi[58], C. Glaser[61], T. Glauch[27], T. Glüsenkamp[26, 61], N. Goehlke[32], J. G. Gonzalez[44], S. Goswami[58], D. Grant[24], S. J. Gray[19], O. Gries[1], S. Griffin[40], S. Griswold[52], K. M. Groth[22], C. Günther[1], P. Gutjahr[23], C. Haack[26], A. Hallgren[61], R. Halliday[24], L. Halve[1], F. Halzen[40], H. Hamdaoui[55], M. Ha Minh[27], K. Hanson[40], J. Hardin[15], A. A. Harnisch[24], P. Hatch[33], A. Haungs[31], K. Helbing[62], J. Hellrung[11], F. Henningsen[27], L. Heuermann[1], N. Heyer[61], S. Hickford[62], A. Hidvegi[54], C. Hill[16], G. C. Hill[2], K. D. Hoffman[19], S. Hori[40], K. Hoshina[40, 66], W. Hou[31], T. Huber[31], K. Hultqvist[54], M. Hünnefeld[23], R. Hussain[40], K. Hymon[23], S. In[56], A. Ishihara[16], M. Jacquart[40], O. Janik[1], M. Jansson[54], G. S. Japaridze[5], M. Jeong[56], M. Jin[14], B. J. P. Jones[4], D. Kang[31], W. Kang[56], X. Kang[49], A. Kappes[43], D. Kappesser[41], L. Kardum[23], T. Karg[63], M. Karl[27], A. Karle[40], U. Katz[26], M. Kauer[40], J. L. Kelley[40], A. Khatee Zathul[40], A. Kheirandish[34, 35], J. Kiryluk[55], S. R. Klein[8, 9], A. Kochocki[24], R. Koirala[44], H. Kolanoski[10], T. Kontrimas[27], L. Köpke[41], C. Kopper[26], D. J. Koskinen[22], P. Koundal[31], M. Kovacevich[49], M. Kowalski[10, 63], T. Kozynets[22], J. Krishnamoorthi[40, 64], K. Kruiswijk[37], E. Krupczak[24], A. Kumar[63], E. Kun[11], N. Kurahashi[49], N. Lad[63], C. Lagunas Gualda[63], M. Lamoureux[37], M. J. Larson[19], S. Latseva[1], F. Lauber[62], J. P. Lazar[14, 40], J. W. Lee[56], K. Leonard DeHolton[60], A. Leszczyńska[44], M. Lincetto[11], Q. R. Liu[40], M. Liubarska[25], E. Lohfink[41], C. Love[49], C. J. Lozano Mariscal[43], L. Lu[40], F. Lucarelli[28], W. Luszczak[20, 21], Y. Lyu[8, 9], J. Madsen[40], K. B. M. Mahn[24], Y. Makino[40], E. Manao[27], S. Mancina[40, 48], W. Marie Sainte[40], I. C. Mariş[12], S. Marka[46], Z. Marka[46], M. Marsee[58], I. Martinez-Soler[14], R. Maruyama[45], F. Mayhew[24], T. McElroy[25], F. McNally[38], J. V. Mead[22], K. Meagher[40], S. Mechbal[63], A. Medina[21], M. Meier[16], Y. Merckx[13], L. Merten[11], J. Micallef[24], J. Mitchell[7], T. Montaruli[28], R. W. Moore[25], Y. Morii[16], R. Morse[40], M. Moulai[40], T. Mukherjee[31], R. Naab[63], R. Nagai[16], M. Nakos[40], U. Naumann[62], J. Necker[63], A. Negi[4], M. Neumann[43], H. Niederhausen[24], M. U. Nisa[24], A. Noell[1], A. Novikov[44], S. C. Nowicki[24], A. Obertacke Pollmann[16], V. O'Dell[40], M. Oehler[31], B. Oeyen[29], A. Olivas[19], R. Ørsøe[27], J. Osborn[40], E. O'Sullivan[61], H. Pandya[44], N. Park[33], G. K. Parker[4], E. N. Paudel[44], L. Paul[42, 50], C. Pérez de los Heros[61], J. Peterson[40], S. Philippen[1], A. Pizzuto[40], M. Plum[50], A. Pontén[61], Y. Popovych[41], M. Prado Rodriguez[40], B. Pries[24], R. Procter-Murphy[19], G. T. Przybylski[9], C. Raab[37], J. Rack-Helleis[41], K. Rawlins[3], Z. Rechav[40], A. Rehman[44], P. Reichherzer[11], G. Renzi[12], E. Resconi[27], S. Reusch[63], W. Rhode[23], B. Riedel[40], A. Rifaie[1], E. J. Roberts[2], S. Robertson[8, 9], S. Rodan[56], G. Roellinghoff[56], M. Rongen[26], C. Rott[53, 56], T. Ruhe[23], L. Ruohan[27], D. Ryckbosch[29], I. Safa[14, 40], J. Saffer[32], D. Salazar-Gallegos[24], P. Sampathkumar[31], S. E. Sanchez Herrera[24], A. Sandrock[62], M. Santander[58], S. Sarkar[25], S. Sarkar[47], J. Savelberg[1], P. Savina[40], M. Schaufel[1], H. Schieler[31], S. Schindler[26], L. Schlickmann[1], B. Schlüter[43], F. Schlüter[12], N. Schmeisser[62], T. Schmidt[19], J. Schneider[26], F. G. Schröder[31, 44], L. Schumacher[26], G. Schwefer[1], S. Sclafani[19], D. Seckel[44], M. Seikh[36], S. Seunarine[51], R. Shah[49], A. Sharma[61], S. Shefali[32], N. Shimizu[16], M. Silva[40], B. Skrzypek[14], B. Smithers[4], R. Snihur[40], J. Soedingrekso[23], A. Søgaard[22], D. Soldin[32], P. Soldin[1], G. Sommani[11], C. Spannfellner[27], G. M. Spiczak[51], C. Spiering[63], M. Stamatikos[21], T. Stanev[44], T. Stezelberger[9], T. Stürwald[62], T. Stuttard[22], G. W. Sullivan[19], I. Taboada[6], S. Ter-Antonyan[7], M. Thiesmeyer[1], W. G. Thompson[14], J. Thwaites[40], S. Tilav[44], K. Tollefson[24], C. Tönnis[56], S. Toscano[12], D. Tosi[40], A. Trettin[63], C. F. Tung[6], R. Turcotte[31], J. P. Twagirayezu[24], B. Ty[40], M. A. Unland Elorrieta[43], A. K. Upadhyay[40, 64], K. Upshaw[7], N. Valtonen-Mattila[61], J. Vandenbroucke[40], N. van Eijndhoven[13], D. Vannerom[15], J. van Santen[63], J. Vara[43], J. Veitch-Michaelis[40], M. Venugopal[31], M. Vereecken[37], S. Verpoest[44], D. Veske[46], A. Vijai[19], C. Walck[54], C. Weaver[24], P. Weigel[15], A. Weindl[31], J. Weldert[60], C. Wendt[40], J. Werthebach[23], M. Weyrauch[31], N. Whitehorn[24], C. H. Wiebusch[1], N. Willey[24], D. R. Williams[58], L. Witthaus[23], A. Wolf[1], M. Wolf[27], G. Wrede[26], X. W. Xu[7], J. P. Yanez[25], E. Yildizci[40], S. Yoshida[16], R. Young[36], F. Yu[14], S. Yu[24], T. Yuan[40], Z. Zhang[55], P. Zhelnin[14], M. Zimmerman[40]

[1] III. Physikalisches Institut, RWTH Aachen University, D-52056 Aachen, Germany
[2] Department of Physics, University of Adelaide, Adelaide, 5005, Australia
[3] Dept. of Physics and Astronomy, University of Alaska Anchorage, 3211 Providence Dr., Anchorage, AK 99508, USA
[4] Dept. of Physics, University of Texas at Arlington, 502 Yates St., Science Hall Rm 108, Box 19059, Arlington, TX 76019, USA
[5] CTSPS, Clark-Atlanta University, Atlanta, GA 30314, USA
[6] School of Physics and Center for Relativistic Astrophysics, Georgia Institute of Technology, Atlanta, GA 30332, USA
[7] Dept. of Physics, Southern University, Baton Rouge, LA 70813, USA
[8] Dept. of Physics, University of California, Berkeley, CA 94720, USA
[9] Lawrence Berkeley National Laboratory, Berkeley, CA 94720, USA
[10] Institut für Physik, Humboldt-Universität zu Berlin, D-12489 Berlin, Germany
[11] Fakultät für Physik & Astronomie, Ruhr-Universität Bochum, D-44780 Bochum, Germany
[12] Université Libre de Bruxelles, Science Faculty CP230, B-1050 Brussels, Belgium

[13] Vrije Universiteit Brussel (VUB), Dienst ELEM, B-1050 Brussels, Belgium
[14] Department of Physics and Laboratory for Particle Physics and Cosmology, Harvard University, Cambridge, MA 02138, USA
[15] Dept. of Physics, Massachusetts Institute of Technology, Cambridge, MA 02139, USA
[16] Dept. of Physics and The International Center for Hadron Astrophysics, Chiba University, Chiba 263-8522, Japan
[17] Department of Physics, Loyola University Chicago, Chicago, IL 60660, USA
[18] Dept. of Physics and Astronomy, University of Canterbury, Private Bag 4800, Christchurch, New Zealand
[19] Dept. of Physics, University of Maryland, College Park, MD 20742, USA
[20] Dept. of Astronomy, Ohio State University, Columbus, OH 43210, USA
[21] Dept. of Physics and Center for Cosmology and Astro-Particle Physics, Ohio State University, Columbus, OH 43210, USA
[22] Niels Bohr Institute, University of Copenhagen, DK-2100 Copenhagen, Denmark
[23] Dept. of Physics, TU Dortmund University, D-44221 Dortmund, Germany
[24] Dept. of Physics and Astronomy, Michigan State University, East Lansing, MI 48824, USA
[25] Dept. of Physics, University of Alberta, Edmonton, Alberta, Canada T6G 2E1
[26] Erlangen Centre for Astroparticle Physics, Friedrich-Alexander-Universität Erlangen-Nürnberg, D-91058 Erlangen, Germany
[27] Technical University of Munich, TUM School of Natural Sciences, Department of Physics, D-85748 Garching bei München, Germany
[28] Département de physique nucléaire et corpusculaire, Université de Genève, CH-1211 Genève, Switzerland
[29] Dept. of Physics and Astronomy, University of Gent, B-9000 Gent, Belgium
[30] Dept. of Physics and Astronomy, University of California, Irvine, CA 92697, USA
[31] Karlsruhe Institute of Technology, Institute for Astroparticle Physics, D-76021 Karlsruhe, Germany
[32] Karlsruhe Institute of Technology, Institute of Experimental Particle Physics, D-76021 Karlsruhe, Germany
[33] Dept. of Physics, Engineering Physics, and Astronomy, Queen's University, Kingston, ON K7L 3N6, Canada
[34] Department of Physics & Astronomy, University of Nevada, Las Vegas, NV, 89154, USA
[35] Nevada Center for Astrophysics, University of Nevada, Las Vegas, NV 89154, USA
[36] Dept. of Physics and Astronomy, University of Kansas, Lawrence, KS 66045, USA
[37] Centre for Cosmology, Particle Physics and Phenomenology - CP3, Université catholique de Louvain, Louvain-la-Neuve, Belgium
[38] Department of Physics, Mercer University, Macon, GA 31207-0001, USA
[39] Dept. of Astronomy, University of Wisconsin–Madison, Madison, WI 53706, USA
[40] Dept. of Physics and Wisconsin IceCube Particle Astrophysics Center, University of Wisconsin–Madison, Madison, WI 53706, USA
[41] Institute of Physics, University of Mainz, Staudinger Weg 7, D-55099 Mainz, Germany
[42] Department of Physics, Marquette University, Milwaukee, WI, 53201, USA
[43] Institut für Kernphysik, Westfälische Wilhelms-Universität Münster, D-48149 Münster, Germany
[44] Bartol Research Institute and Dept. of Physics and Astronomy, University of Delaware, Newark, DE 19716, USA
[45] Dept. of Physics, Yale University, New Haven, CT 06520, USA
[46] Columbia Astrophysics and Nevis Laboratories, Columbia University, New York, NY 10027, USA
[47] Dept. of Physics, University of Oxford, Parks Road, Oxford OX1 3PU, United Kingdom
[48] Dipartimento di Fisica e Astronomia Galileo Galilei, Università Degli Studi di Padova, 35122 Padova PD, Italy
[49] Dept. of Physics, Drexel University, 3141 Chestnut Street, Philadelphia, PA 19104, USA
[50] Physics Department, South Dakota School of Mines and Technology, Rapid City, SD 57701, USA
[51] Dept. of Physics, University of Wisconsin, River Falls, WI 54022, USA
[52] Dept. of Physics and Astronomy, University of Rochester, Rochester, NY 14627, USA
[53] Department of Physics and Astronomy, University of Utah, Salt Lake City, UT 84112, USA
[54] Oskar Klein Centre and Dept. of Physics, Stockholm University, SE-10691 Stockholm, Sweden
[55] Dept. of Physics and Astronomy, Stony Brook University, Stony Brook, NY 11794-3800, USA
[56] Dept. of Physics, Sungkyunkwan University, Suwon 16419, Korea
[57] Institute of Physics, Academia Sinica, Taipei, 11529, Taiwan
[58] Dept. of Physics and Astronomy, University of Alabama, Tuscaloosa, AL 35487, USA
[59] Dept. of Astronomy and Astrophysics, Pennsylvania State University, University Park, PA 16802, USA
[60] Dept. of Physics, Pennsylvania State University, University Park, PA 16802, USA
[61] Dept. of Physics and Astronomy, Uppsala University, Box 516, S-75120 Uppsala, Sweden
[62] Dept. of Physics, University of Wuppertal, D-42119 Wuppertal, Germany
[63] Deutsches Elektronen-Synchrotron DESY, Platanenallee 6, 15738 Zeuthen, Germany
[64] Institute of Physics, Sachivalaya Marg, Sainik School Post, Bhubaneswar 751005, India
[65] Department of Space, Earth and Environment, Chalmers University of Technology, 412 96 Gothenburg, Sweden
[66] Earthquake Research Institute, University of Tokyo, Bunkyo, Tokyo 113-0032, Japan

Acknowledgements

The authors gratefully acknowledge the support from the following agencies and institutions: USA – U.S. National Science Foundation-Office of Polar Programs, U.S. National Science Foundation-Physics Division, U.S. National Science Foundation-EPSCoR, Wisconsin Alumni Research Foundation, Center for High Throughput Computing (CHTC) at the University of Wisconsin–Madison, Open Science

Grid (OSG), Advanced Cyberinfrastructure Coordination Ecosystem: Services & Support (ACCESS), Frontera computing project at the Texas Advanced Computing Center, U.S. Department of Energy-National Energy Research Scientific Computing Center, Particle astrophysics research computing center at the University of Maryland, Institute for Cyber-Enabled Research at Michigan State University, and Astroparticle physics computational facility at Marquette University; Belgium – Funds for Scientific Research (FRS-FNRS and FWO), FWO Odysseus and Big Science programmes, and Belgian Federal Science Policy Office (Belspo); Germany – Bundesministerium für Bildung und Forschung (BMBF), Deutsche Forschungsgemeinschaft (DFG), Helmholtz Alliance for Astroparticle Physics (HAP), Initiative and Networking Fund of the Helmholtz Association, Deutsches Elektronen Synchrotron (DESY), and High Performance Computing cluster of the RWTH Aachen; Sweden – Swedish Research Council, Swedish Polar Research Secretariat, Swedish National Infrastructure for Computing (SNIC), and Knut and Alice Wallenberg Foundation; European Union – EGI Advanced Computing for research; Australia – Australian Research Council; Canada – Natural Sciences and Engineering Research Council of Canada, Calcul Québec, Compute Ontario, Canada Foundation for Innovation, WestGrid, and Compute Canada; Denmark – Villum Fonden, Carlsberg Foundation, and European Commission; New Zealand – Marsden Fund; Japan – Japan Society for Promotion of Science (JSPS) and Institute for Global Prominent Research (IGPR) of Chiba University; Korea – National Research Foundation of Korea (NRF); Switzerland – Swiss National Science Foundation (SNSF); United Kingdom – Department of Physics, University of Oxford.